Electric Vehicle Charging System with PV Grid-Connected Configuration

Experimental tests of control and power management

Fabrice Locment, Manuela Sechilariu
AVENUES Team Research
University of Technology of Compiegne
Compiegne, France
fabrice.locment@utc.fr

Christophe Forgez
LEC EA 1006
University of Technology of Compiegne
Compiegne, France

Abstract—**This paper presents an experimental control strategy of electric vehicle charging system composed of photovoltaic (PV) array, converters, power grid emulator and programmable DC electronic load that represents Li-ion battery emulator. The designed system can supply the battery at the same time as PV energy production. The applied control strategy aims to extract maximum power from PV array and manages the energy flow through the battery with respect to its state of charge and taking into account the constraints of the public grid. The experimental results, obtained with a dSPACE 1103 controller board, show that the system responds within certain limits and confirm the relevance of such system for electric vehicle charging.**

Keywords-renewable energy integration, photovoltaic, battery electric vehicles, public grid, control charging system.

I. INTRODUCTION

Improved quality of life and increased mobility lead to greater consumption of energy resources and implied greenhouse gas emissions. This increased power consumption involves more quality and reliability to regulate electricity flows, less mismatching between electricity generation and demand, and more integrated renewable energies. Thus, the concept of smart grid is born in recent years. A smart grid could be easily defined as the electricity delivery system, which transports, converts and distributes the power efficiently (from producers to consumers), integrated with communications and information technology. The main goal of smart grid is to assist in balancing the power generation and the power consumption using sensors, communications and monitoring technologies. Then, the smart grid is seen as a set formed by the interaction of three layers: power transportation and distribution layer, communication and sensors layer and software applications and services layer.

Considering tomorrow's electric needs like electric cars, balancing the electricity demand and electricity production in order to increase the grid efficiency while decreasing the number of power outages, is a real huge challenge. In fact, plug-in hybrid electric vehicles (PHEVs) and electric vehicles (EVs) represent an important step in solving environmental problems and are being developed around the world. Many studies are going on to optimize engine and battery efficiency for both operations discharge and recharge. However, it is important to understand the further impact of PHEVs and mostly EVs recharging operation on the electric grid [1] [2]. Depending on when and where the vehicles are plugged in, they could cause strongly constraints on the grid. The expectation is that the grid will not be seriously affected because the recharging would mostly occur during the night hours. Nevertheless, the end-users preference to plug in when convenient for them, rather than utility grid would prefer, may be stronger.

On the other hand, the renewable and distributed electricity share of the energy mix is increasing, and its grid integration associated to an energy management system is more than ever necessary. Hence, one solution, from an environmental standpoint, is that the PHEVs and EVs are wholly or partially charged from a renewable energy source [3] [4] [5]. Today it is difficult to give an average of typical autonomy for EVs between recharges. Several manufacturers announced for soon EVs with an autonomy range of several tens of km. Given the high mobility existing today, it is likely that an EV driver needs to recharge the vehicle during his stay to work, whence the possibility of recharging with photovoltaic (PV) energy during the daylight. In urban areas, there is a favourable politico-economic context, which leads to a significant development of small PV power plant, therefore associated or integrated to tertiary or residential building and car parking. Today, green energy purchase conditions lead quite naturally these applications to a grid-connected system with a total and permanent energy injection. However, having regard to the technical constraints due to the absence of the smart grid who should integrate energy management, this development could be restrained by the power back grid capacity. Ideally, electricity must be consumed at the moment it is generated, particularly true with peak demand, with minimum electric losses along the power lines from the power generation to end-consumer. In this context, for buildings, car parking and charging stations equipped with PV power plant, the system that allows the EVs charging directly from the PV power and a bidirectional energy flow from/to the grid is an alternative solution to those technical difficulties. This system is a PV power local generation, whose energy produced is intended priority for self-feeding, with a grid connection for further

supply in case of need and for sale of excess energy. By means of a smart meter, this system's grid connection would take into account the availability, needs and vulnerability of the electric grid. A smart meter is able to communicate information via some network back to the public grid for monitoring and billing purpose.

This paper focuses on PV grid-connected system control strategy, which allows the feeding of a battery electric vehicle (*BEV*) at the same time and in the same place as the energy PV production. First, the system is presented as several subsystems: PV array, power grid emulator and programmable DC electronic load, which imposes currents in order to simulate the functioning of a Li-ion *BEV*. The system control aims to extract maximum power from PV array and manages the power transfer through the battery load, with respect to its state of charge (SOC) and taking into account the public grid availability and needs. In order to transfer to the *BEV*, at every moment, the maximum PV power available, a maximum power point tracking (MPPT) strategy is introduced. The MPPT algorithm is Incremental Conductance [6] [7] and aims to find in real time the current reference for which PV would provide the maximum of its power. In order to simulate correctly the Li-ion *BEV* charging, a voltage control is implemented within the respect of an adequate SOC. The experimental results obtained with a dSPACE 1103 controller board show that the system responds within certain limits and confirm the relevance of such configuration for EVs charging system.

II. Electric Vehicle Charging System

Many small PV systems operate in grid-connected mode which involves no interaction with a local load. The proposed system allows both connections, with *BEV*, as load, and public grid.

A. General System Overview

The EVs charging system with PV grid-connected configuration is presented on the Fig. 1. It is a matter of PV local power generation with an integrated energy management system operating under the assumption that the locally generated power is used where, when, and how it is generated. The public grid is used only as a backup and if available. That could eliminate energy consumption from the utility grid by means of self-feeding and sale the excess power only if the public grid allows it. Thus, for more energy efficiency, the generated electricity must be consumed in the production form; this is why we take into consideration the development of *BEVs* charging points.

When the sunshine is too weak to generate the entire necessary power to transfer to the *BEVs,* the public grid supplies the DC load also. In contrast, when the generated PV power is more important than the *BEVs* demanded power, the system sends power back to the grid. The bidirectional energy flow from/to the grid is operated taking into account the public grid availability and needs. For this, an experimental platform and a test bench have been installed in our university, whose images are given on the Fig. 2. It refers mainly to 16 PV panels ($2kW_P$, Fig. 2(a)), a weather station, a public grid emulator

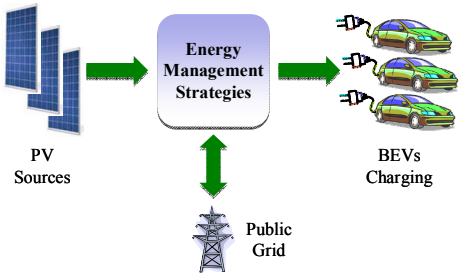

Figure 1. EVs charging station with PV grid-connected system.

Figure 2. (a) Image of PV array, (b) test bench.

(linear amplifier 3kVA), a dSPACE 1103 controller board, and power electronics necessary. This system is associated with a programmable DC electronic load (Chroma 63202, 2.6kW 500V-50A) that allows simulating the typical *BEV* charging cycle, Fig. 2(b).

B. PV Array Configuration

The PV array (*PVA*) is composed of 16 PV panels Solar Fabrik SF-130/2-125, and its electrical specifications are presented in Table I. The electrical coupling is given on the Fig. 3. There are two serial set of four parallel branches formed by two series PV panels.

TABLE I. Electrical STC specifications of PV panel

Solar-Fabrik SF-130/2-125	
N_S number of cells in series	36
I_{SC}, short-circuit current	7.84A
V_{OC}, open-circuit voltage	21.53V
I_{MPP}, maximum power point current	7.14A
V_{MPP}, maximum power point voltage	17.50V
K_0 temperature coefficient for current	0.00545A/K
Θ^* temperature reference	298K
g^* solar irradiance reference	1000W/m²

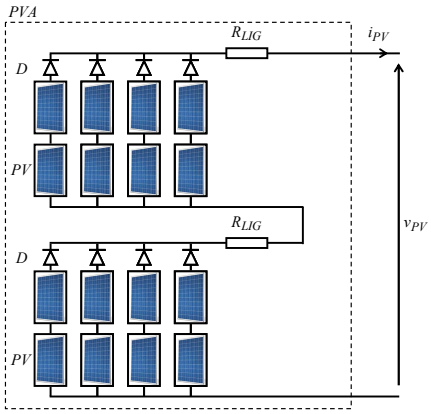

Figure 3. PV panels electrical coupling.

In order to protect the PV panels from the run-back current, one diode D is placed in the head of each branch. Resistance line, which represents power line losses, is symbolized by R_{LIG}.

C. Electrical system description

The *BEV* charging system, illustrated on the Fig. 4, consists of 4-leg power converter (B_1 to B_4), *PVA* described earlier, *BEV* emulator, public grid (*PG*) emulator and a set of inductors and capacitors in order to ensure compatibility between the different elements. The studied system is divided in several subsystems.

1) PVA and impedance adapter subsystem

PVA is electrically coupled to the DC bus through the B_1 power converter leg and the L_{PV} inductance. Equations (1) model the described *PVA* and impedance adapter subsystem:

$$\frac{di_{PV}}{dt} = \frac{1}{L_{PV}}\left(v_{PV} - v'_{PV}\right)$$

$$\begin{bmatrix} i'_{PV} \\ v'_{PV} \end{bmatrix} = a_{PV}\begin{bmatrix} i_{PV} \\ v \end{bmatrix} \tag{1}$$

$$a_{PV} = \frac{1}{T}\int_0^T f_{B1}\,dt\,,\ a_{PV} \in [0;1]$$

The power supplied by *PVA* depends on the solar irradiance (g), PV cell temperature (θ), array voltage (v_{PV}) and the current through the *PVA* (i_{PV}).

The operating point of a load connected at the PV generator does not coincide always with the optimal point and varies according to the weather conditions. In order to maximize the produced energy from the *PVA*, the INcremental Conductance (INC) MPPT method is proposed to find and maintain the peak power.

The INC MPPT algorithm uses the derivative of the PV system conductance in order to determine the operating point position in relation to maximum power point (MPP).

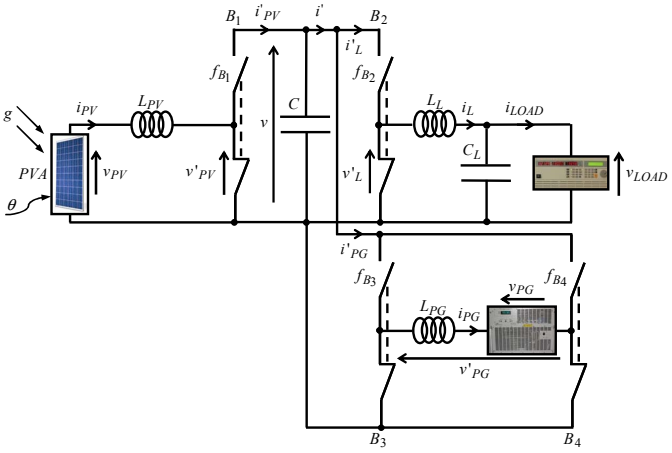

Figure 4. *BEV* charging electrical scheme.

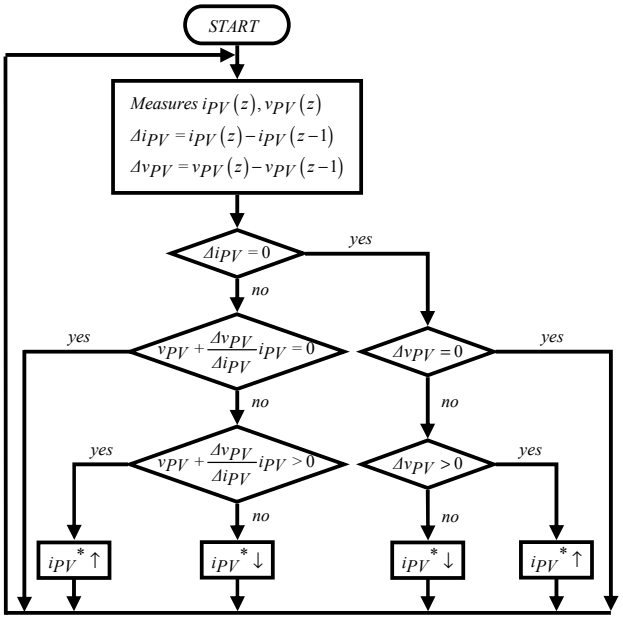

Figure 5. Flow chart of the INC algorithm.

In this work, this procedure is performed in order to impose the current reference i_{PV}^*. As in [8], it is based on the fact that the slope tangent of the characteristic $p_{PV} - i_{PV}$ ($p_{PV} = v_{PV}\ i_{PV}$) is zero in MPP, positive on the MPP left side, and negative on the MPP right side. So, the derivate of the *PVA* impedance $\frac{dv_{PV}}{di_{PV}}$ is used.

$$di_{PV} \approx \Delta i_{PV} = i_{PV}(z) - i_{PV}(z-1)$$
$$dv_{PV} \approx \Delta v_{PV} = v_{PV}(z) - v_{PV}(z-1) \tag{2}$$

From the instantaneous measurement of i_{PV} and v_{PV}, and assuming (2) with z and z-1 measurement instants, the algorithm can instantly calculate $\frac{v_{PV}}{i_{PV}}$ and $\frac{dv_{PV}}{di_{PV}}$ to deduct the direction of perturbation leading to the MPP. This is done by acting on i_{PV}^*. Fig. 5 shows the flow chart of the INC algorithm.

2) DC Bus subsystem

The DC bus consists of a C capacitor and an electrical coupling of v voltage. The operating DC bus equations are:

$$\frac{dv}{dt} = \frac{1}{C}\left(i'_{PV} - i'\right)$$
$$i' = i'_{PG} + i'_L \tag{3}$$

3) Battery Electric Vehicle Emulator subsystem

The Li-ion battery is assumed to be charged with a so-called CC/CV procedure [9]. This one consists to charge a Li-ion battery in two modes, a constant current (CC) mode followed by a constant voltage (CV) mode. During the CC

mode, the charging current stays constant until the voltage rises to a cut-off voltage. In our case, this voltage is 3.6V per cell. It is assumed that all the cells of the battery pack are balanced by a battery management system. During the CV mode, the voltage remains constant while the current drops. A CC/CV procedure has been applied to an A123 LiFePO4 26650 cell and recorded. In order to emulate the *BEV* charge, a CC/CV profile proportional to the profile recorded on one cell is considered.

The Li-ion battery is emulated by imposing the current in the load (i_{LOAD}) and by controlling the voltage across the capacitor (v_{LOAD}). The behaviour of a Li-ion battery pack for a typical charging cycle is emulated by means of a programmable DC electronic load. The *BEV* current reference i^*_{LOAD} (Fig. 6) and *BEV* voltage reference v^*_{LOAD} (Fig. 7) are obtained by coupling 100 cells in series.

Fig. 6 shows the comparison between i^*_{LOAD} and i_{LOAD}, whose evolutions are identically, except the end of the charging that corresponds to the programmable DC electronic load behaviour for low current values. Regarding the voltage evolution, both reference voltage v^*_{LOAD} and load voltage v_{LOAD} are identically as presented on Fig. 7.

The *BEV* emulator is electrically coupled to the DC bus through the B_2 power converter leg, L_L inductance and C_L capacitor. The modelling equations are given by (4).

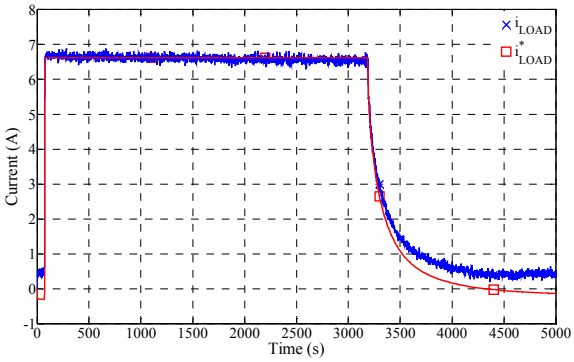

Figure 6. *BEV* current mode charge.

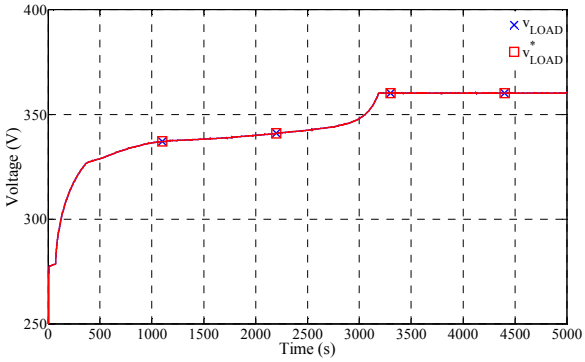

Figure 7. *BEV* voltage mode charge.

$$\begin{aligned} \frac{di_L}{dt} &= \frac{1}{L_L}(v'_L - v_{LOAD}) \\ \frac{dv_{LOAD}}{dt} &= \frac{1}{C_L}(i_L - i_{LOAD}) \\ \begin{bmatrix} i'_L \\ v'_L \end{bmatrix} &= a_L \begin{bmatrix} i_L \\ v \end{bmatrix} \\ a_L = \frac{1}{T}\int_0^T f_{B2}\,dt\,,\ a_L &\in [0;1] \end{aligned} \tag{4}$$

4) Public Grid Emulator subsystem

The PG is electrically coupled to the DC bus through the B_3 and B_4 power converter legs and the L_{PG} inductance. This connection is necessary for the bidirectional energy flow.

The DC bus voltage v is secured thanks to this subsystem. The operating equations are given by (5).

$$\begin{aligned} \frac{di_{PG}}{dt} &= \frac{1}{L_{PG}}(v'_{PG} - v_{PG}) \\ \begin{bmatrix} i'_{PG} \\ v'_{PG} \end{bmatrix} &= a_{PG} \begin{bmatrix} i_{PG} \\ v_{PG} \end{bmatrix} \\ a_{PG} = \frac{1}{T}\int_0^T (f_{B3} - f_{B4})\,dt \ \text{ with } \ f_{B3} &= \overline{f_{B4}} \\ a_{PG} &\in [-1;1] \end{aligned} \tag{5}$$

III. CONTROL SYSTEM STRATEGY

The system control strategy aims to extract maximum power from *PVA* and manages the power transfer through the *BEV* with the respect to its SOC.

By means of three settings ($a_{PV}{}^*$, $a_L{}^*$ and $a_{PG}{}^*$) five state variables (i_{PV}, v, i_L, v_{LOAD} and i_{PG}) are controlled. In order to control this system, the principles of direct and indirect inversion are applied: direct inversion (without controller) for items that are not time functions, indirect inversion (with controller) for items that are time functions.

The reference current $i_{PV}{}^*$ is obtained following the INC MPPT strategy. The adopted control is performed according to $a_{PV}{}^*$ setting described by (6):

$$a_{PV}{}^* = \frac{-C_{PV}\left(i_{PV}{}^* - i_{PV}\right) + v_{PV}}{v} \tag{6}$$

As experimentally the voltage v_{PV} is very noisy, this voltage is not subject to feedback control. Controller C_{PV} is proportional integral type.

According to the CC/CV charging procedure of the *BEV* emulator described earlier, a nested current loop with voltage loop is necessary. This control leads to following equations:

$$a_L{}^* = \frac{C_{LI}\left(i_L{}^* - i_L\right) + v_{LOAD}}{v} \quad \text{with}$$
$$i_L{}^* = C_{LV}\left(v_{LOAD}{}^* - v_{LOAD}\right) + i_{LOAD} \tag{7}$$

Controller C_{LI} and C_{LV} are proportional because voltage v_{LOAD} and current i_{LOAD} are experimentally compensated. In order to ensure the properly running of the system the nested current-voltage loops have to be correctly uncoupled using C_{LI} and C_{LV} controllers' bandwidths; the current inner loop bandwidth is much larger than the voltage outer loop.

The last setting is:

$$a_{PG}{}^* = \frac{C_{PGI}\left(i_{PG}{}^* - i_{PG}\right) + v_{PG}}{v} \tag{8}$$

Controller C_{PGI} is proportional integral as C_{PV}. In order to define $i_{PG}{}^*$, the security system must be described. In this case, the security system is achieved by DC bus voltage control. Thus, DC bus current adjustment i'^* is defined by:

$$i'^* = -C_{PGV}\left(v^* - v\right) + i'_{PV} \tag{9}$$

where C_{PGV} is the same corrector like C_{PGI}, with the same setting.

From (3) and (9), the following expression is obtained:

$$i'_{PG}{}^* = -C_{PGV}\left(v^* - v\right) + i'_{PV} - i'_L \tag{10}$$

The currents i'_{PV} and i'_L are experimentally very noisy, and they are not subject to feedback control. Thus, neglecting the total losses of B_3 and B_4 power converter legs and L_{PG} inductor losses, (10) could be transformed in (11):

$$i_{PG}{}^* = \frac{v}{v_{PG}}\left(-C_{PGV}\left(v^* - v\right) + i'_{PV} - i'_L\right) \tag{11}$$

For all controllers, synthesis for correction is not realized in this study.

IV. Experimental Results and Discussion

The objective of this work is more to validate a comprehensive approach rather than purely numerical results. For this reason, we do not give the numerical values of various system components studied. All the implemented automatic controls, described earlier, are working satisfactorily although simplifying assumptions regarding losses were made.

The SOC by CC/CV mode charging compared to reference SOC*, obtained from i^*_{LOAD} and v^*_{LOAD}, is shown on Fig. 8. Both SOC and SOC* evolutions are identically, except the end of the charge that corresponds to the programmable DC electronic load behaviour for low current values. For this comprehensive system approach, it is considered that these results allow accepting the simulation of the typical *BEV* charging cycle by means of the programmable DC electronic load.

The experimental results of the EV charging system with PV grid-connected configuration are presented on Fig. 9 for a solar irradiance g evolution on March 10th in 2010 starting from 1:30 pm at Compiegne, France.

The experimental test results are given within the following powers expressions: $p_{PV} = v_{PV}\, i_{PV}$ power provided by the *PVA*, $p_{LOAD} = v_{LOAD}\, i_{LOAD}$ power requested by the *BEV*, and $p_{PG} = v_{PG}\, i_{PG}$ public grid transfer power. Fig. 9 shows the solar irradiance g evolution and EV charging system powers evolutions. Firstly, it is shown that the implemented INC MPPT algorithm works correctly according to p_{PV} proportional to solar irradiance g.

For the period taken into account, we observe that the strategy outlined earlier is well respected. For $p_{PV} < p_{LOAD}$ the public grid provides energy, in contrast it receives. Regarding the security system, whatever the sign and the amplitude of the difference of powers between p_{PV} and p_{LOAD}, these results show that this experimental system runs safety.

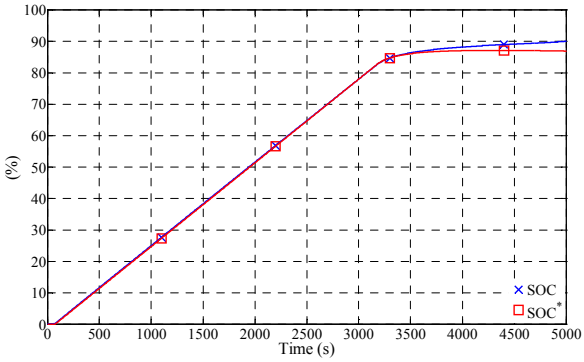

Figure 8. *BEV* SOC and reference SOC*.

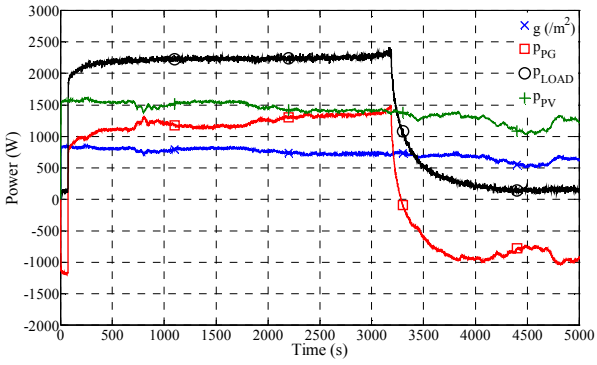

Figure 9. Solar irradiance g evolution on March 10th in 2010 starting from 1:30 pm at Compiegne and EV charging system powers evolutions (p_{PV} supplied by PV system versus g solar iradiance, p_{LOAD} absorbed by *BEV*, and p_{PG} for public grid).

Although correctors involve improvements to minimize perturbations, the DC bus voltage remains at a constant value. In the other hand, from the balance of powers, system losses are observed. These ones are not the object of this study but they must certainly be taken into account for improving the EV charging system energy efficiency.

In conclusion, it is observed that the overall system, as has been designed, responds satisfactorily within the outlined strategy.

Concerning the system's grid connection, the availability, needs and vulnerability of the electric grid should be taken into account. Let us suppose that in the future smart grid, a special smart device, via some network, is able to receive information from the public grid and is able to send back information also. This public grid monitoring could inform the described experimental system about the public grid real time needs.

Thus, in order to inform correctly the system about the public grid availability, a very simple method could be to introduce in (11) a coefficient K_{PG} with $K_{PG} \in \{0,1\}$. Equation (11) is transformed in (12):

$$i_{PG}{}^{*} = K_{PG} \cdot \frac{v}{v_{PG}} \left(-C_{PGV} \left(v^{*} - v \right) + i'_{PV} - i'_{L} \right) \qquad (12)$$

For public grid unrestricted availability $K_{PG} = 1$ and either case $p_{PV} > p_{LOAD}$ or $p_{PV} < p_{LOAD}$, the EV charging system operates as highlighted.

For public grid unavailability $K_{PG} = 0$ and $p_{PV} > p_{LOAD}$, the EV charging system operates under very limited conditions linked to capacitor C sizing. In this case, some additional storage means must be introduced in the system. For $p_{PV} < p_{LOAD}$ the *sine qua non* operating requirement of the EV charging system is to add sources like storage [10], micro-cogeneration unit (green gas, wood-pellets or sterling engines), or fuel cell. Also, public grid restricted availability control must be well designed. There could be matter of "only supply" or "only injection", even more fully or partially supply or injection, which involve calculated values of K_{PG} corresponding to public grid conditions and also unidirectional control of B_3 and B_4 power converter legs.

V. CONCLUSION

Smart grid with renewable electricity integrated concerns both the utility companies as well as the end-users. In the next ten years, the smart grid could concern the residential level with house power "routers", whose goal is to intelligently manage and supply every home appliance by minimizing and redirecting the overall consumption. The prime goal of utility companies could be the real time demand management in order to adjust their electricity generation, for end user it could be the real time control of energy use, like EV charging system.

An experimental EV charging with PV grid-connected system control strategy was presented. The system control strategy aims to extract maximum power from PV array and manages the energy flow through the *BEV*, with respect to its SOC. The experimental results are obtained with a numerical modelling implemented under MATLAB-Simulink and a dSPACE 1103 controller board. In this work, a simple and quick to implement control was done. This control was not necessarily developed to improve global energy efficiency or life cycle of the *BEV* system. For this first approach, the goal was to verify the feasibility of the proposed system control.

The results show that the system can supply a *BEV* at the same time as PV energy production and responds within certain limits of the PV power and public grid availability. Obtained test results indicate that the proposed control can successfully be used for buildings and car parking equipped with PV power plant.

The further work is the modelling of the behaviour of EV charging with PV grid-connected system as an operating subsystem under the supervision device as a control-command subsystem. The chosen approach will take into account the uncertainties on PV power production, public grid availability and *BEV* request, in order to achieve more efficient power transfer with a minimized public grid impact.

REFERENCES

[1] S. D. Jenkins, J. R. Rossmaier, and M. Ferdowsi, "Utilization and effect of plug-in hybrid electric vehicles in the United States power grid", in: *Proc. IEEE Vehicle Power and Propulsion Conference, VPPC 2008*.

[2] EPRI, "Environmental Assessment of Plug-In Hybrid Electric Vehicles; Volume 1: Nationwide Greenhouse Gas Emissions", Final Report, July 2007.

[3] V. Marano and G. Rizzoni, "Energy and Economic Evaluation of PHEVs and their Interaction with Renewable Energy Sources and the Power Grid", in: *Proc. IEEE International Conference on Vehicular Electronics and Safety*, 2008.

[4] Y. Gurkaynak and A. Khaligh, "Control and Power Management of a Grid Connected Residential Photovoltaic System with Plug-in Hybrid Electric Vehicle (PHEV) Load", in *Proc. IEEE Applied Power Electronics Conference and Exposition*, *APEC 2009*.

[5] X. Li, L. A. C. Lopes, and S. S. Williamson, "On the suitability of plug-in hybrid electric vehicle (PHEV) charging infrastructures based on wind and solar energy", in: *Proc. IEEE Power & Energy Society General Meeting, PES 2009.*

[6] V. Salas, E. Olias, A. Barrado, and A. Lazaro, "Review of the maximum power point tracking algorithms for stand-alone photovoltaic systems", *Solar Energy Materials and Solar Cells* 90-11, pp. 1555-1578, 2006.

[7] T. Esram and P. L. Chapman, "Comparison of photovoltaic array maximum power point tracking techniques", *IEEE Transactions on Energy Conversion* 22-2, pp. 439, 2007.

[8] I. Houssamo, F. Locment and M. Sechilariu. "Maximum power tracking for photovoltaic power system: Development and experimental comparison of two algorithms*", Renewable Energy* 35-10, pp. 2381-2387, 2010.

[9] H. J. Bergveld, P. H. L. Notten, W. S. Kruijt, "Battery management systems: design by modeling", Kluwer Academic Publishers, 2002.

[10] M. Sechilariu, F. Locment and I. Houssamo. "Multi-Source Power Generation System in Semi-isolated and Safety Grid Configuration for Buildings », in: *Proc. IEEE Mediteranean Electrotechnical Conference MELECON 2010*.